Extragalactic Star Clusters
IAU Symposium Series, Vol. 207, 2002
Doug Geisler, Eva K. Grebel, and Dante Minniti, eds.

The Infrared Luminosity Function in the 30 Dor Cluster

Hans Zinnecker & Morten Andersen

Astrophysikalisches Institut Potsdam, Germany

Bernhard Brandl

Cornell University, Ithaca, USA

Wolfgang Brandner

ESO Garching, Germany

Deidre Hunter

Lowell Observatory, Flagstaff, USA

Richard Larson

Yale Astronomy Department, New Haven, USA

Mark McCaughrean

Astrophysikalisches Institut Potsdam, Germany

Georges Meylan

STScI, Baltimore, USA

Andrea Moneti

Institut d'Astrophysique, Paris, France

Abstract. We present the first infrared luminosity function in the 30 Doradus star cluster obtained with the HST NIC1 camera ($0.043''$ pixel^{-1}) in the F160W (H-band) filter. Despite diffraction limited resolution ($0.15''$), crowding and blending is so severe that the cluster centre R136 cannot be studied. Instead a neighbouring NIC1 field (about $15''$ away from the centre), for which an empirical PSF could be obtained, was analysed. We obtained photometry for some 750 stars in the range H = 14 to 22 mag. The luminosity function continues rising up to H = 21 mag (1 $M_{\odot}$ at an age of 2 Myr) after which incompleteness corrections become dramatic (exceeding 50 %). Contrary to recent optical studies based on a V vs. V–I diagram (Sirianni et al. 2000), we do not infer a flattening or turnover of the implied IMF slope near 2 $M_{\odot}$.

https://doi.org/10.1017/S0074180900224340 Published online by Cambridge University Press

1. Introduction

At a distance of 50 kpc in the LMC, 30 Doradus is the biggest and most luminous H II region in the Local Group (e.g., Kennicutt & Chu 1994). It covers an area of 200 pc × 200 pc and emits some 10^{52} Lyman continuum photons s^{-1}. Its exciting star cluster, NGC2070, has a radius of about 20 pc and contains some 50 very massive ($> 50\ M_{\odot}$) stars (Melnick 1985), most of them in a compact core (named R136) of radius 2 pc. The very central object R136a was once believed to be a single supermassive star, but high-spatial resolution optical speckle observations resolved it into 8 individual luminous stars (Weigelt & Baier 1985; Pehlemann et al. 1992). Subsequently, Hubble Space Telescope (HST) WFPC1/2 and FOS observations (Hunter et al. 1995, 1996; Massey & Hunter 1998), and near-IR adaptive optics observations (Brandl et al. 1996), further resolved and clarified the high- and intermediate-mass stellar content of the R136 cluster. It was found that the number of high mass stars is in good agreement with the number of intermediate mass stars, suggesting that a Salpeter-like IMF holds over the whole main sequence mass range of $3 - 120\, M_{\odot}$ within the R136 cluster. Recently, Sirianni et al. (2000) reanalysed the archival HST WFPC2 data (V vs. V–I) pushing a magnitude deeper, i.e., into the regime of pre-main sequence stars, and identified a population of red stars evenly distributed around the R136 cluster. These authors constructed an IMF in the $1.5 - 6.5\, M_{\odot}$ range, taking incompleteness into account, and claimed that the IMF shows a definite flattening below $2\, M_{\odot}$.

Here we present new data taken with the infrared camera NICMOS aboard HST to show that the infrared luminosity function outside the R136 core down to $H = 21$ mag ($\sim 1\, M_{\odot}$ at age 2 Myr) in fact does *not* indicate any signs of flattening and appears to keep rising to fainter magnitudes. The reasons to go to the near-IR include the need to minimise extinction problems and the expectation to detect the fainter cool stars when trying to reveal the low-mass pre-main sequence population.

2. HST/NICMOS observations

We used the NIC2 camera (FOV $19.2'' \times 19.2''$) to obtain a 3×3 position mosaic of the central square-arcmin (15 pc× 15 pc) of the R136 cluster in the F160W filter. This mosaic is shown in Figure 1. Observations with the NIC1 camera (spatial resolution $0.15''$, sampled at $0.043''$ per pixel) were obtained in parallel and with the same filter. Here we concentrate on a single NIC1 field (FOV $11.2'' \times 11.2''$, 2.8 pc × 2.8 pc) located $15''$ from the cluster centre (see box in Figure 1). In a previous report, we analysed a 3×1 position NIC2 mosaic extending radially from $20 - 60''$ ($15 - 25$ pc) which we called Wing-2 (Zinnecker et al. 1999).

3. Data Reduction

The NIC1 data were processed with the standard HST/NICMOS pipeline and the four dithered images at each position were then drizzled together. The source detection was done using the DAOFIND program and the photometry was done with the ALLSTAR program. The empirical PSF for the PSF-photometry was created from less crowded fields than the one shown; it is displayed in Figure 3, together with the nice spider (Tarantula) resembling both 30 Dor (also known as the Tarantula Nebula) and the PSF. A 7-step process was employed to iteratively subtract the brightest stars at each step, down to 6 sigma objects. In the process the nebulosity was also removed. The calibration from counts to magnitudes was done according to the guide on the NICMOS homepage. Photometry for some 750 objects in the range $H = 14 - 22$ mag was obtained.

4. Results

Figure 4 shows the NIC1 H-band luminosity function, including the incompleteness corrections that we derived from artificial star experiments (Monte Carlo simulations). The extinction correction in the infrared H-band is small (< 0.5 mag), i.e., smaller than our bin size, and has been neglected here. We see that the infrared luminosity function keeps rising steadily to $H = 20$ mag, and notice that incompleteness starts to become important beyond $H = 20$ mag. At $H = 21$ mag we derive incompleteness factors of 1.5, indicating that the luminosity function becomes unreliable at fainter magnitudes. Thus we believe that we can trust our infrared luminosity function in 30 Dor to $H = 21$ mag, i.e., absolute magnitude $M_H = 2.5$, for a distance modulus to the LMC of 18.5 mag. $M_H = 2.5$ corresponds to $\sim 1\,M_\odot$ at an age of 2 Myr (D'Antona & Mazzitelli 1994; Palla & Testi, personal communication). However, it is worth noting that at least some sources are detected in the $H = 22.0 - 22.5$ mag bin, which would correspond to pre-main sequence stars of about $0.5\,M_\odot$.

The slope of the luminosity function in Figure 4 is ~ 0.35, which for a 2 Myr coeval low-mass pre-main sequence stellar population ($M \leq 3\,M_\odot$) corresponds very closely to a Salpeter IMF with index $\Gamma = 1.4$, the same as Hunter et al. (1995, 1996) found for the higher mass stars ($M \geq 3\,M_\odot$). Thus we find no evidence for a break in the slope of the IMF down to $1\,M_\odot$, contrary to the analysis of Sirianni et al. (2000) using optical HST data. The suggestion is that the inferred flattening in the IMF derived from optical data may be a selection effect, which disappears in the near-infrared, where extinction becomes insignificant in this cluster. This is in line with earlier deep infrared H- and K-band adaptive optics results in the south-eastern quadrant of R136 (Brandl et al. 1996) which, when combined with Hunter et al. optical HST data, clearly showed a star to star extinction variation, with A_V ranging from 1 to 3 mag and demonstrating the limits of optical data when deducing the slope of the IMF near the magnitude limit (see also Selman et al. 1999).

In summary, we find no evidence so far for an unusual IMF in the R136 cluster, which is often considered the closest example of a true starburst.

https://doi.org/10.1017/S0074180900224340 Published online by Cambridge University Press

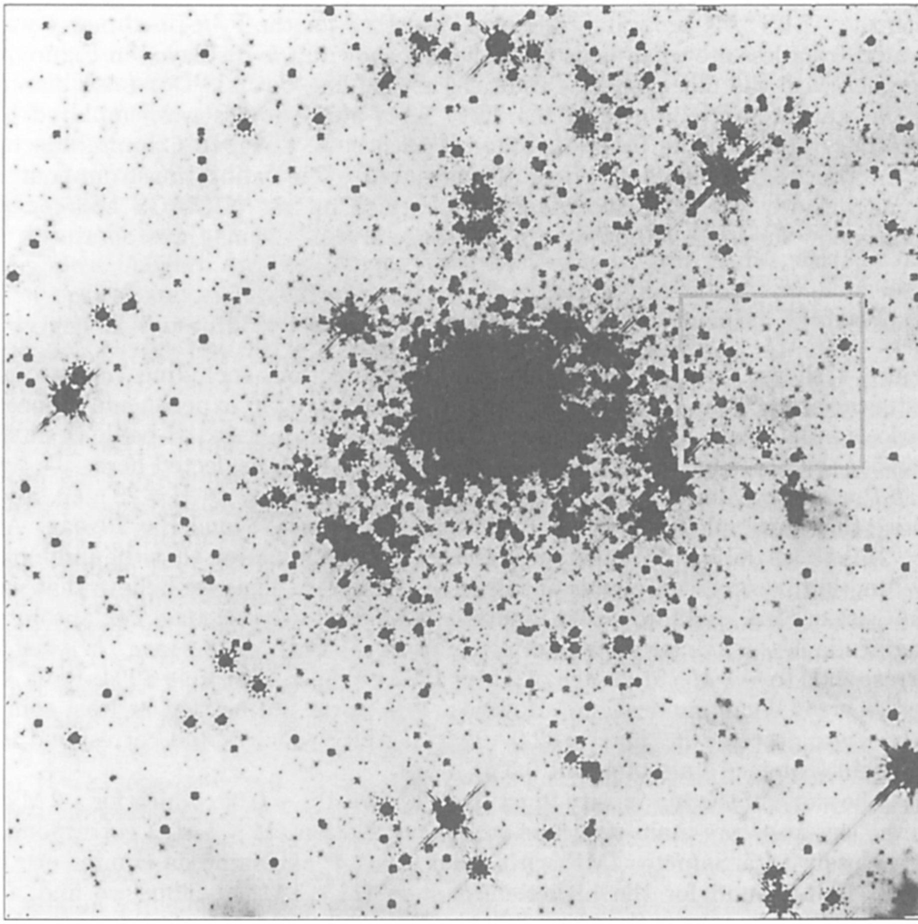

Figure 1. HST NIC2 F160W image of the R136 cluster (FOV $\sim 1\,\mathrm{arcmin} \times 1\,\mathrm{arcmin}$). The box next to the cluster core indicates the region observed in parallel with NIC1 and analysed here. Seen from the centre, north is towards the upper right corner, east towards the upper left corner.

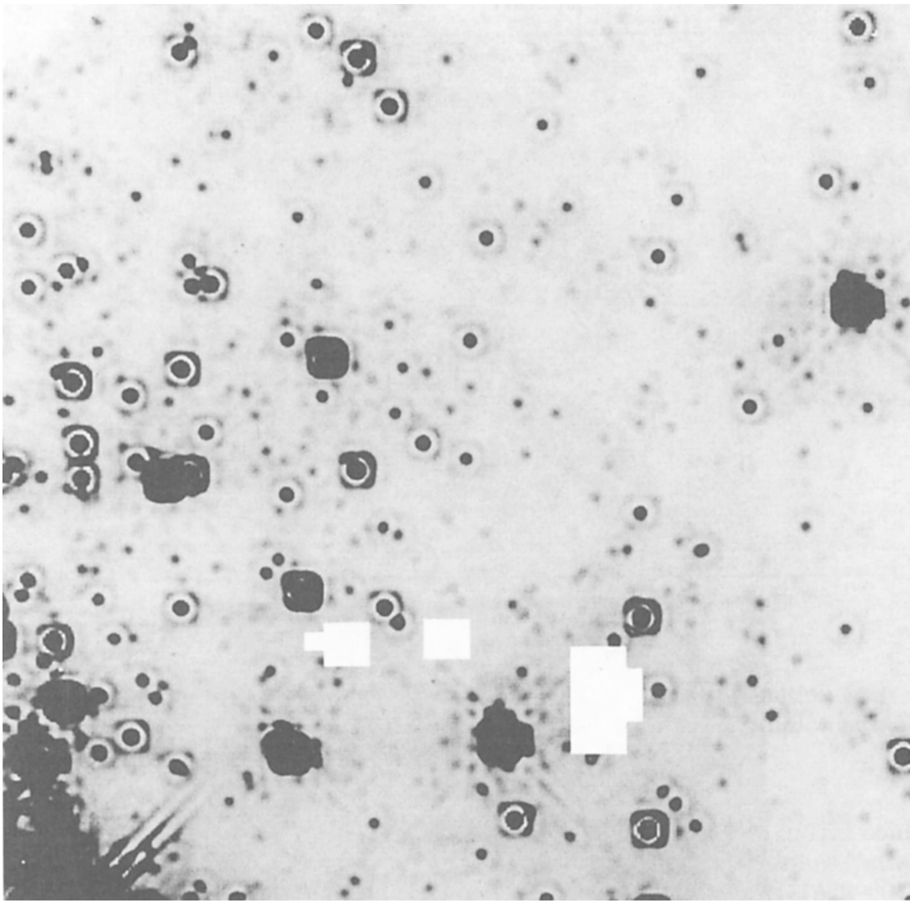

Figure 2. HST NIC1 F160W image of the region (FOV $\sim 10'' \times 10''$) outlined in Figure 1. The white areas have been masked and are not considered in the analysis due to persistence effects from very bright stars imaged at prevous positions in the mosaic.

https://doi.org/10.1017/S0074180900224340 Published online by Cambridge University Press

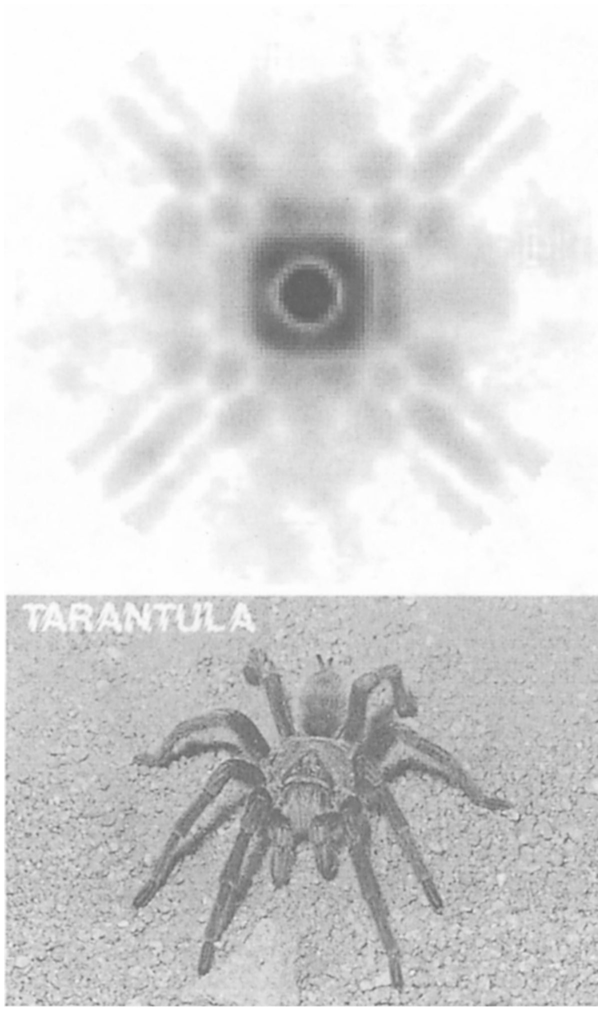

Figure 3. Empirical NIC1 F160W point spread function (top). The scaling is logarithmic, and the radius of the circular area is 33 pixels or 1.42″. Tarantula spider (bottom) for comparison with the PSF and the Tarantula Nebula.

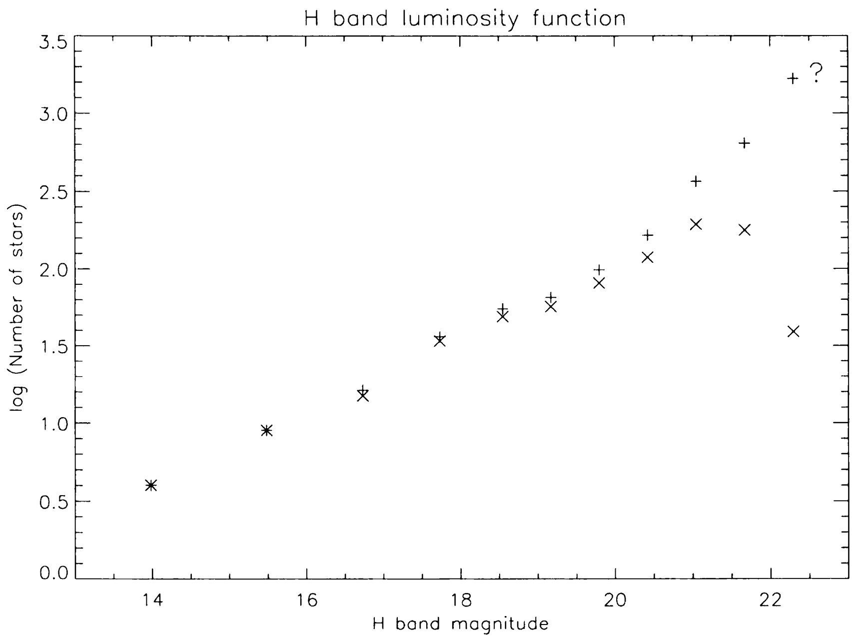

Figure 4. H-band (F160W filter) infrared luminosity function (×) of the NIC1 field shown in Figure 2. Note the incompleteness corrections (+).

Acknowledgments. This research and H. Z.'s participation in this conference were supported by the European Commission Research Training Network on "The Formation and Evolution of Young Stellar Clusters" (RTN–1999–00436, HPRN–CT–2000–00155). M.A.'s participation was made possible through a grant from the LOC and the Astronomische Gesellschaft for which he is grateful. Both of us very much enjoyed being part of this first IAU Symposium in Chile and congratulate the organizers for an exceptional meeting in an exceptional location (Pucón).

References

Brandl, B. et al. 1996, ApJ, 466, 254

Brandner, W. et al. 2001, AJ, 122, 858

D'Antona, F., & Mazzitelli, I. 1994, ApJS, 90, 467

Hunter, D. A. et al. 1995, ApJ, 448, 179

Hunter, D. A. et al. 1996, ApJ, 459, L27

Kennicutt, R. C., & Chu, Y.-H. 1994, in Violent Star Formation, ed. G. Tenorio-Tagle (Cambridge: Cambridge Univ. Press), 1

Massey, P., & Hunter, D. A. 1998, ApJ, 493, 180

Melnick, J. 1985, A&A, 153, 235

https://doi.org/10.1017/S0074180900224340 Published online by Cambridge University Press

Pehlemann, E., Hofmann, K.-H., & Weigelt, G. 1992, A&A, 256, 701

Selman, F. et al. 1999, A&A, 347, 532

Sirianni, M. et al. 2000, ApJ, 533, 203

Weigelt, G., & Baier, G. 1985, A&A, 150, L18

Zinnecker, H. et al. 1999, in IAU-Symp. 190, New Views of the Magellanic Clouds, ed. Y.-H. Chu, N. Suntzeff, J. Hesser, & D. Bohlender (San Francisco: ASP), 222

Discussion

M. Sirianni: In our investigation, the final combined image in F555W has been subdivided into four regions surrounding the R136 cluster, with the objective of establishing the completeness of our photometry. The four regions display different characteristics of crowding and/or gas/dust contamination. We have used an average of three (homogeneous) regions, to derive the completeness correction factors for our photometry and from this a completeness histogram as a function of luminosity and then mass. Our 75 % completeness limit lies near $2\,M_\odot$, our 50 % completeness limit near $1.35\,M_\odot$.

W. Brandl: In response to Sirianni's comment, note that avoiding areas of patchy extinction does *not* solve the problem of the so-called magnitude limit correction (Selman et al. 1999; see also Brandner et al. 2001). What counts is the individual stellar reddening which can be quite significant for pre-MS stars.

D. Geisler: What are your thoughts on the origin of 30 Doradus?

H. Zinnecker: You mean the star cluster associated with 30 Doradus. Well, I think what you need is a very compact initial configuration of gas, of order 10^5 solar masses of gas packed into the space of 1 cubic-parsec. The escape velocity from such a dense neutral gas cloud is about 20 km/s, in excess of the sound speed of the same amout of gas when it has become ionized (10 km/s). Therefore the original compact gas cloud survives ionization due to the massive stars that form, and we have a gravitationally trapped H II region. The real question of course is how to get such a dense gaseous system in the first place, and my answer is that it appears that the collision of two or three gaseous supershells in the LMC (see Fukui's contribution) may have swept together and compressed the gas into this dense and compact proto-globular cluster configuration.

J. Melnick: Is there any need for LMC field star corrections?

H. Zinnecker: No. The cluster is so dense that this does not matter. The probability of a red giant star in our field is of order 10 %, as estimated by Brandl et al. in their 1996 paper (section 4.2.2).